



# Self-Updating Local Variogram Models using Automatic Clustering in Iterative Geostatistical Seismic Inversion

Shaghayegh Esmaeilzadeh, Ali Moradzadeh\*, Reza Mohebian, and Omid Asghari

School of Mining Engineering, College of Engineering, University of Tehran, Tehran, Iran

## Article Info

Received 3 January 2025

Received in Revised form 17 February 2025

Accepted 6 March 2025

Published online 6 March 2025

DOI: [10.22044/jme.2025.15541.2978](https://doi.org/10.22044/jme.2025.15541.2978)

## Keywords

Stochastic inversion

Local spatial continuity models

Direct sequential simulation

Self-learning

Hierarchical clustering

## Abstract

Seismic inversion is a critical technique for estimating the spatial distribution of petro-elastic properties in the subsurface, based on the seismic reflection data. This work introduces an iterative geostatistical seismic inversion method, designed to address challenges in complex geological settings by incorporating self-updating local variogram models. Unlike the conventional approaches that rely on a single global variogram or fixed local variograms, the proposed method dynamically updates the spatial continuity models at each iteration using automatic variogram modeling and clustering of variogram parameters. The optimal number of clusters is determined using three cluster validity indices: Silhouette Index (SI), Davies-Bouldin Index (DB), and Calinski-Harabasz Index (CH). The method's effectiveness was evaluated using a three-dimensional non-stationary synthetic dataset, demonstrating robust convergence when employing the SI and CH indices, with both achieving a high global correlation coefficient of 0.9 between the predicted and true seismic data. Among these, the CH index provided the best balance between the computational efficiency and inversion accuracy. The results highlight the method's ability to effectively capture local spatial variability, while maintaining a reasonable computational cost, making it a promising approach for seismic inversion in complex sub-surface environments.

## 1. Introduction

Seismic inversion derives the spatial distribution of subsurface petro-elastic properties from recorded seismic reflection data. It is a complex, ill-posed, and highly non-linear problem with non-unique solutions, typically solved using deterministic or probabilistic approaches [1-3]. Deterministic methods provide a single solution that represents the best estimate or most likely value of the model parameters. In contrast, probabilistic algorithms yield solutions in the form of probability distributions for the variables of interest, expressed as either conditional probability density functions or model realizations conditioned on the data. Unlike deterministic approaches, probabilistic methods quantify the uncertainty associated with the solution [1, 4]. Within this framework, two primary methods that are commonly used to address the seismic inversion problem: Bayesian-linearized approaches [e.g., 5,

6-8], and geostatistical seismic inversion [e.g., 9, 10-15].

Iterative geostatistical seismic inversion methods employ stochastic sequential simulation and co-simulation, combined with a global optimizer, to perturb and update the model parameter space. Unlike the Bayesian linearized methods, stochastic inversion does not rely on pre-defined parametric distributions, allowing for a more comprehensive parameter space exploration. However, this comes with increased computational costs, due to the absence of analytical solutions [1, 10].

Geostatistical seismic inversion faces challenges in complex geological settings, where it can produce geologically unrealistic inverted models. This issue arises primarily because the spatial continuity of subsurface properties is often modeled using a single global variogram, which

✉ Corresponding author: [a\\_moradzadeh@ut.ac.ir](mailto:a_moradzadeh@ut.ac.ir) (A. Moradzadeh)

may not accurately reflect true geological variability. To address this, multiple regionalized variogram models that capture local spatial continuity patterns can be employed in iterative geostatistical seismic inversion [e.g., 16, 17]. However, using fixed local variogram models throughout the iterative process risks propagating errors if the assumed spatial continuity model is inaccurate [14]. In this context, Pereira, et al. [14] introduced an iterative approach that updates local variogram models using the template matching technique. This method reduces the limitations of relying on a fixed variogram model, which may not accurately capture spatial variability, and enhances the estimation of local anisotropies in complex geological settings. However, it has only been tested on two-dimensional seismic data, and its high computational cost is a significant drawback—one iteration generating 32 two-dimensional realizations required 93 minutes on an Intel Core i7 workstation with 32 GB of RAM.

This work introduces a self-updating method for local variogram models that integrates the mismatch between predicted and observed seismic data at each iteration of the seismic inversion process. The local variogram models are updated using automatic variogram modeling and automatic clustering of variogram parameters, ensuring an adaptive representation of spatial continuity. In subsequent iterations, the updated variogram models constrain the stochastic sequential co-simulation of new realizations (Figure 1). Unlike Pereira et al.'s method, which has only been applied to two-dimensional seismic data, our approach is designed for testing on three-dimensional seismic inversion, achieving a balance between accuracy and computational efficiency.

A key component of the proposed algorithm is automatic clustering. Clustering is an unsupervised learning technique, used to uncover hidden structures within unlabeled data [18]. It plays a crucial role in analyzing input datasets by grouping

them into clusters, with the optimal number of clusters either pre-defined or automatically determined. In automatic clustering, the process is evaluated using a Cluster Validity Index (CVI), which helps identify the optimal number of clusters in the dataset [19].

Numerous CVIs have been proposed in the literature, and several review studies have compared their effectiveness. For example, Arbelaitz, et al. [20], found that the Silhouette, Davies-Bouldin, and Calinski-Harabasz indices tend to deliver the best performance. In a similar vein, José-García and Gómez-Flores [21] demonstrated that the Silhouette index reliably performs well on linearly separable datasets, while the Calinski-Harabasz, Davies-Bouldin, and generalized Dunn indices show satisfactory results on both synthetic and real-world datasets. Additionally, Ikotun, et al. [22] reported that the Davies-Bouldin index is the most widely used CVI in automatic clustering algorithms.

In contrast to earlier geostatistical seismic inversion methods that rely on fixed global or local variogram models—which often fail to capture true spatial variability in complex geological settings—or employ computationally expensive updating techniques; this study introduces an iterative approach that self-updates local variogram models through automatic clustering. The proposed method overcomes the limitations of traditional approaches by incorporating the mismatch between the predicted and observed seismic data into the inversion process, allowing for an adaptive refinement of local spatial continuity models. Furthermore, our approach is specifically designed for three-dimensional seismic data, achieving these improvements with a reasonable computational cost. To optimize this process, we compared the performance of three cluster validity indices—the Silhouette Index (SI), Davies-Bouldin Index (DB), and Calinski-Harabasz Index (CH)—within our framework.

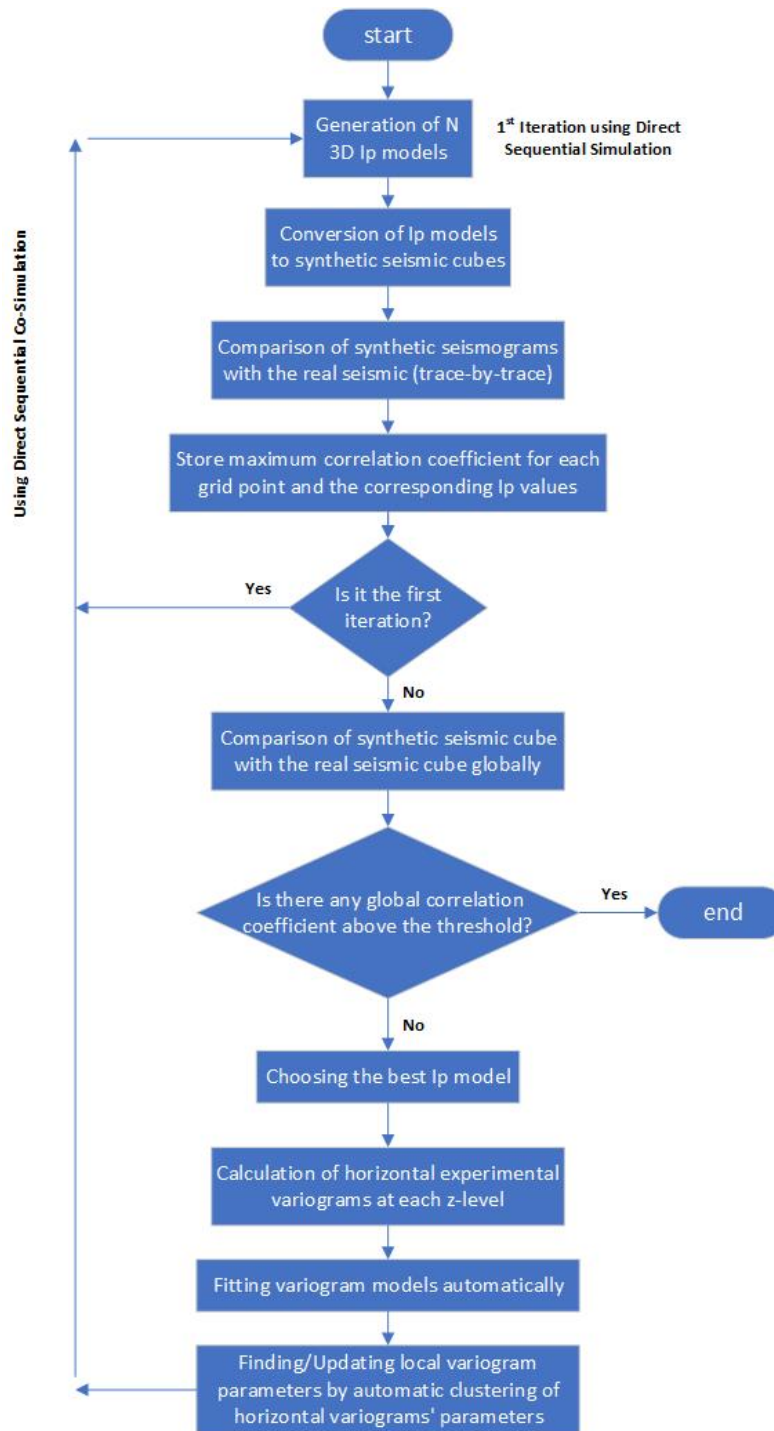


Figure 1. Flowchart of the iterative geostatistical seismic inversion with self-updating local variogram models using automatic clustering.

## 2. Materials and Methods

The method proposed in this work builds upon the Global Stochastic Seismic Inversion (GSI) introduced by Soares, et al. [15]. GSI assumes a stationary spatial continuity pattern, which is rarely applicable in complex geological environments.

This work addresses this limitation by incorporating local variogram models into the model perturbation step. These variogram models are iteratively adjusted based on the data mismatch from the previous iteration. The proposed algorithm can be outlined in the following steps:

1. Use direct sequential simulation [23] to generate a set of three-dimensional acoustic impedance models, employing well-log data as input and a variogram model to describe the spatial continuity pattern.
2. Calculate synthetic seismic reflection volumes for each acoustic impedance model produced in step 1.
3. Compare the synthetic seismic data with the real data on a trace-by-trace basis using the correlation coefficient. Save two supplementary volumes: the best Ip traces and their associated local correlation coefficients.
4. Use the two supplementary volumes as secondary variables and local regionalized models for the co-simulation of a new set of acoustic impedance models.
5. Repeat steps 2 and 3.
6. Select the best acoustic impedance model produced in step 4 by comparing the synthetic seismograms and real seismic data globally.
7. Calculate horizontal experimental variograms at each z-level (depth) of the best acoustic impedance model selected in the previous step.
8. Fit a variogram model to the horizontal experimental variograms calculated at each z-level.
9. Cluster the variogram parameters obtained at each z-level using the z-levels as constraints. This process groups the z-levels into zones, each defined by its own set of local variogram parameters.
10. Co-simulate a new set of acoustic impedance models, as in step 4, but using the local variograms obtained in step 9 instead of a single global variogram.
11. Repeat steps 5 to 10 until a pre-defined number of iterations is completed, or the global correlation coefficient between the real and synthetic seismic volumes exceeds a specified threshold.

The variogram parameters for each z-level (depth) were clustered to identify distinct zones exhibiting similar spatial variability patterns. This was achieved using a hierarchical clustering approach, specifically Ward's linkage method, which minimizes within-cluster variance. To enforce spatial continuity, a significant penalty was applied to non-adjacent data points in the distance matrix, ensuring that clusters consist of contiguous z-levels.

For each identified zone, the variogram parameters (sill, nugget, and horizontal range) were determined by averaging the horizontal variogram parameters of the z-levels within that zone. The vertical range for each zone's variogram was then calculated using the updated horizontal range and a fixed anisotropy ratio. This anisotropy ratio,

defined as the ratio of the horizontal to vertical range in the global variogram, was assumed to remain constant throughout the inversion grid.

The optimal number of clusters, which defines the number of zones, was determined automatically through optimizing a CVI. This work utilized the Silhouette, Davies-Bouldin, and Calinski-Harabasz indices, defined as follows:

$$SI_k = \frac{1}{n} \sum_{i=1}^n \frac{(b_i - a_i)}{\max(a_i, b_i)}, \quad (1)$$

where  $n$  is the total number of data points,  $a_i$  is the average distance from point  $i$  to other points within the same cluster,  $b_i$  is the minimum average distance from point  $i$  to points in a different cluster.

$$DB_k = \frac{1}{k} \sum_{i=1}^k \max_{j \neq i} \left( \frac{s_i + s_j}{d_{ij}} \right), \quad (2)$$

where  $k$  is the number of clusters,  $s_i$  is the average distance between points in cluster  $i$  and the centroid of cluster  $i$ , and  $d_{ij}$  is the distance between the centroids of clusters  $i$  and  $j$ .

$$CH_k = \frac{\text{trace}(B_k)}{\text{trace}(W_k)} \cdot \frac{n - k}{k - 1} \quad (3)$$

where  $\text{trace}(B_k)$  is the trace of the between-cluster dispersion matrix and  $\text{trace}(W_k)$  is the trace of the within-cluster dispersion matrix.

Using different CVIs results in varying numbers of clusters (zones) and different configurations in each iteration of the inversion algorithm, ultimately affecting the final inversion results. Another important consideration is the computational cost that automatic clustering imposes on the inversion algorithm, which varies depending on the CVI used. Given that geostatistical seismic inversion itself incurs significant computational costs, selecting a CVI with an appropriate computational cost is crucial. Therefore, the proposed algorithm was run using each of the CVIs mentioned above, and the resulting inversion outcomes and computational costs were compared, as explained in the following section.

The proposed inversion method was tested on a three-dimensional, non-stationary synthetic full-stack volume. Figure 2 presents three vertical sections extracted from the full-stack volume. This synthetic dataset was designed to replicate the key elastic properties of a real deep-water turbidite field. The inversion grid consists of  $101 \times 101 \times 90$  blocks in the  $i$ -,  $j$ -, and  $k$ -directions, respectively. Each grid cell measures 25 meters in the  $i$  and  $j$  directions, while the size in the vertical direction

corresponds to the seismic sampling rate. The dataset includes 32 wells with Ip-log data. As in real-world cases, the wells were preferentially drilled in reservoir zones, rather than randomly distributed across the grid. The seismic data,

sampled at a 4 ms interval, was generated by stacking angle gathers with a fold of 10, derived using the Zoeppritz equations. The wavelet used in the inversion was the same as that used to generate the synthetic seismic volume.

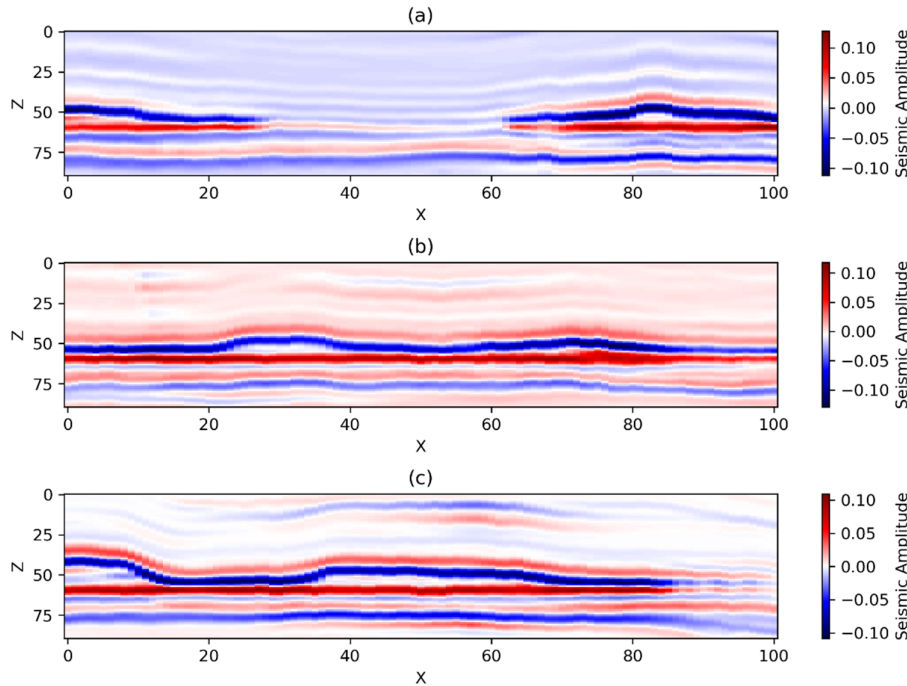


**Figure 2.** Vertical sections extracted from the true full-stack seismic volume at (a)  $y = 25$ , (b)  $y = 50$ , and (c)  $y = 75$ .

In the initial simulations of the proposed method, a global, omnidirectional spherical variogram model was utilized as a starting point. This model was characterized by an isotropic horizontal range of 20 grid cells and a vertical range of 5 grid cells. Following this phase, the approach transitioned to employing local variograms for a more precise representation of the spatial variability of the subsurface properties.

For the local variograms, the model shape remained spherical, while the range, nugget, sill, and the number and thicknesses of zones were iteratively updated based on the mismatch between predicted and observed seismic data. For clustering, the nugget was normalized to the sill, and two horizontal variogram parameters—range and normalized nugget—were used.

### 3. Results and Discussion

The proposed method was applied independently with each of the three clustering validation indices (CVIs): Silhouette Index (SI),

Davies-Bouldin Index (DB), and Calinski-Harabasz Index (CH). For each run, a total of nine sets of simulations were conducted, with each set comprising 64 realizations. The method demonstrated successful convergence when utilizing the SI and CH indices, achieving a high global correlation coefficient of 0.9 between the true and predicted synthetic seismic data. In contrast, the execution employing the DB index failed to exceed a global correlation coefficient of 0.83. These outcomes are illustrated in Figure 3, highlighting the relative effectiveness of the different CVIs in guiding the proposed inversion process.

Furthermore, the proposed method achieved the highest accuracy in reproducing the principal seismic reflection locations and the amplitude content of the true seismic data when using the SI index, followed closely by the CH index. In contrast, the method using the DB index showed the largest discrepancies, with notable mismatches in both reflection locations and amplitude content when compared to the true seismic data (Figure 4).

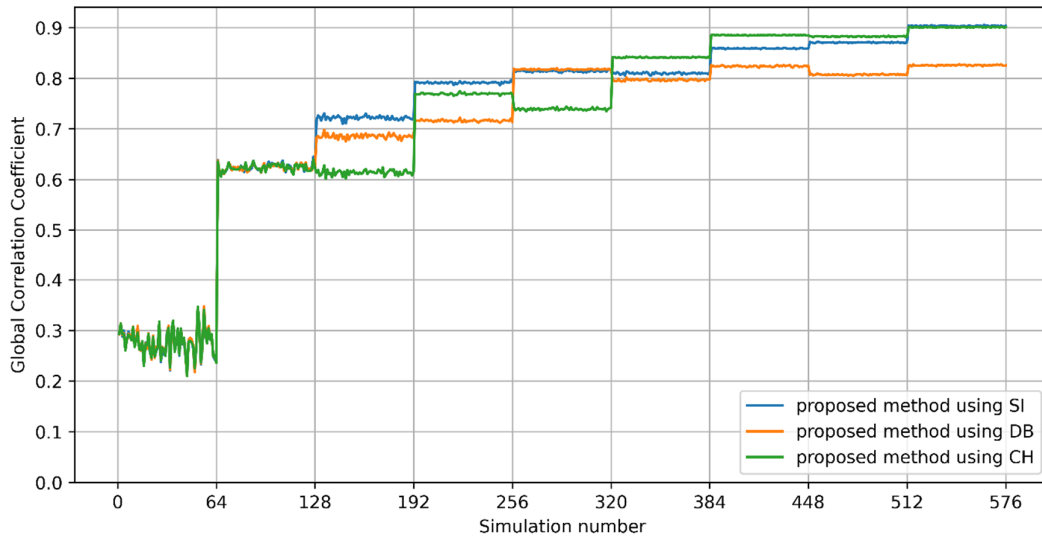


**Figure 3. Evolution of the global correlation coefficient between synthetic and true seismic reflection data for the proposed method using the three CVIs: Silhouette Index (SI), Davies-Bouldin Index (DB), and Calinski-Harabasz Index (CH).**

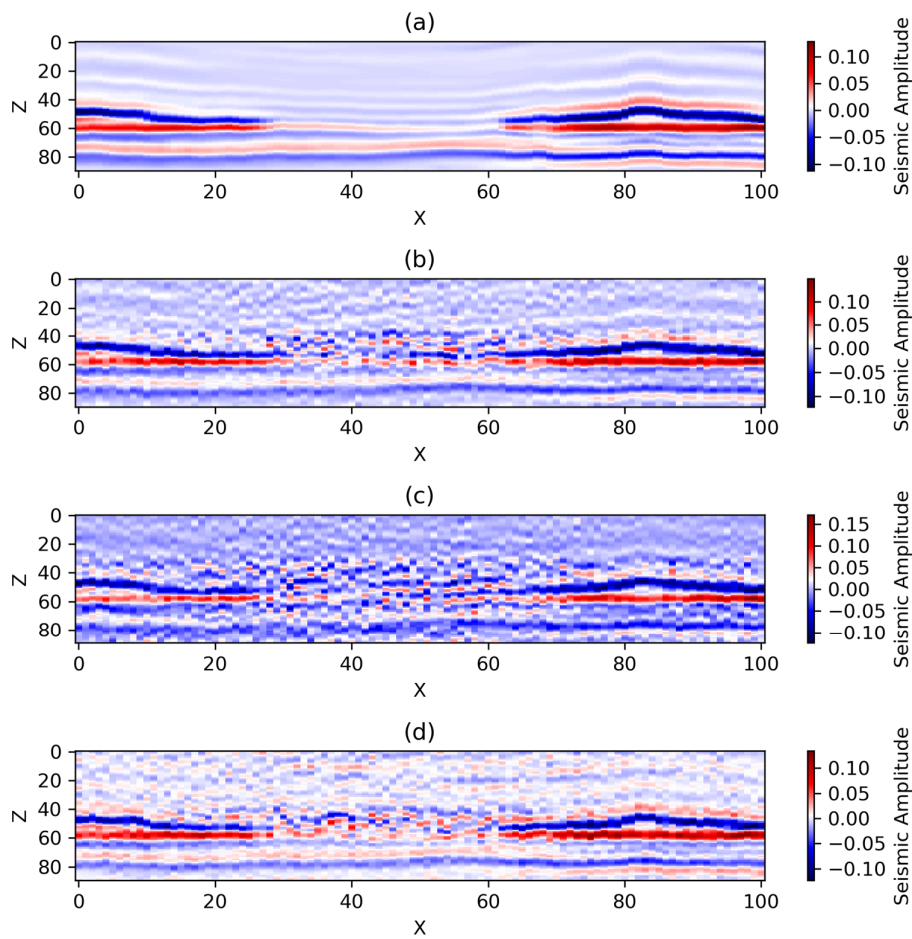


**Figure 4. Vertical sections extracted from (a) the true seismic volume, (b), (c), and (d) synthetic seismic volumes generated from the best-fit inverted acoustic impedance models using the proposed method with the Silhouette Index, Davies-Bouldin Index, and Calinski-Harabasz Index, respectively.**

Achieving a reasonable representation of sub-surface properties in seismic inversion requires more than just a good match between real and synthetic seismic data, because the seismic inversion problem is inherently non-unique, vastly different elastic models can result in identical seismic responses. Figure 5 compares the best-fit acoustic impedance models obtained by the proposed method using SI, DB, and CH indices to the reference acoustic impedance model. The proposed method effectively reproduces the acoustic impedance spatial distribution and values, but the results are significantly better when using SI and CH indices compared to the DB index. To provide a better comparison, the absolute difference between the best-fit acoustic impedance models and the reference model at the same vertical

section shown in Figure 5 is represented in Figure 6.

The final zones, determined by the proposed method after iterative updates to the number and thickness of zones are illustrated in Figure 5 on the vertical sections of the best-fit inverted acoustic impedance. The method ultimately divided the investigated region (entire inversion grid) into three zones, two zones, and four zones along the vertical axis when using the SI, DB, and CH indices, respectively. Tables 1, 2, and 3 present the variogram parameters for each of these final zones, which were applied to co-simulate 64 acoustic impedance models during the final iteration of the proposed method using the SI, DB, and CH indices, respectively.

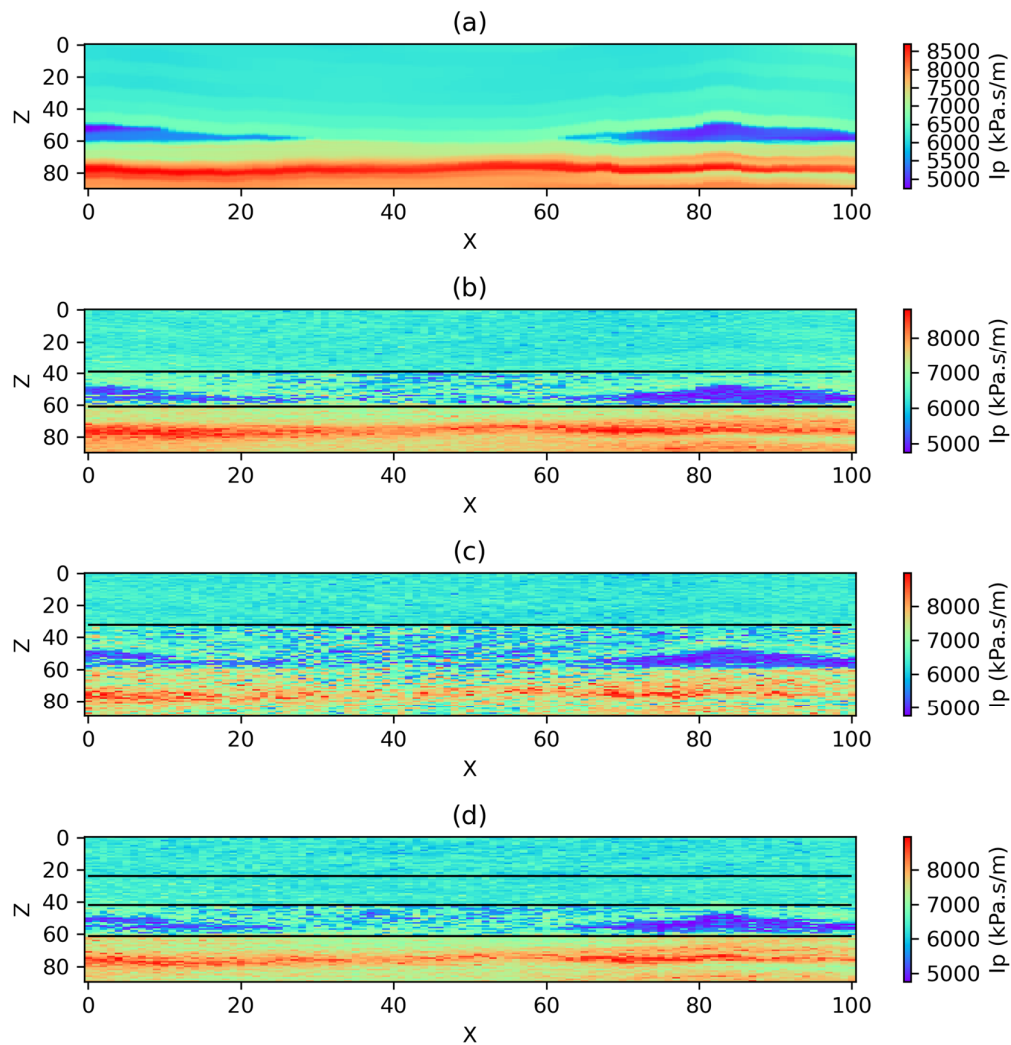


**Figure 5. Vertical sections extracted from (a) the true acoustic impedance ( $I_p$ ) volume, (b), (c), and (d) the best-fit inverted acoustic impedance volumes using the proposed method with the Silhouette Index, Davies-Bouldin Index, and Calinski-Harabasz Index, respectively. The final zonation is separated by horizons shown as thick black lines.**

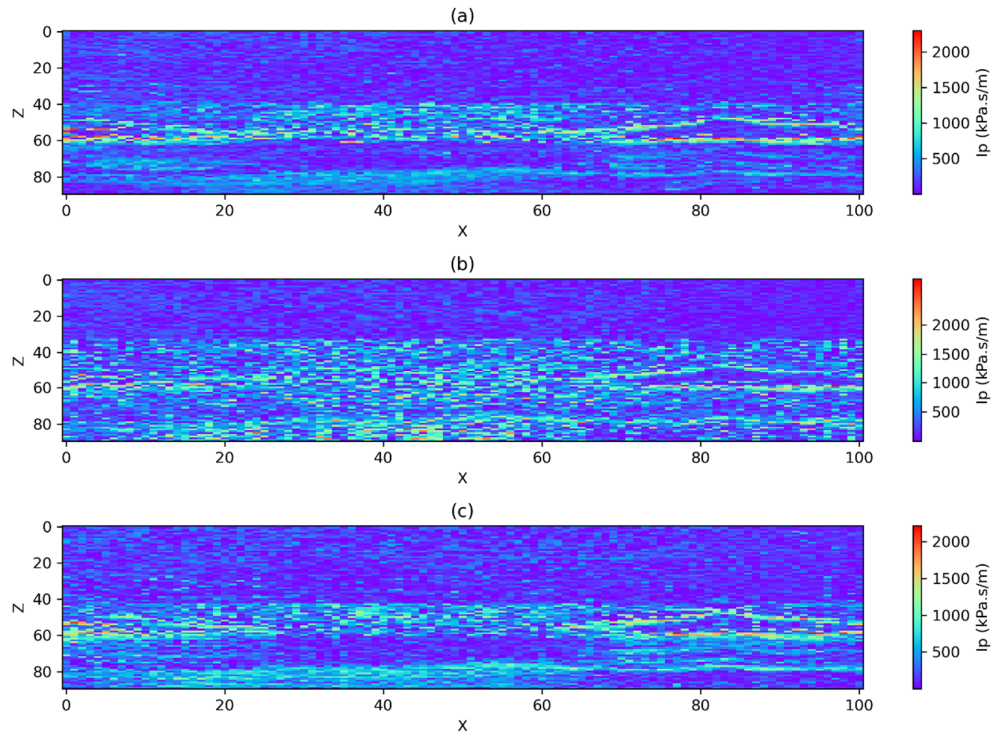


Figure 6. The absolute difference between the true and best-fit inverted acoustic impedance (Ip) models using the proposed method with (a) the Silhouette Index, (b) the Davies-Bouldin Index, and (c) the Calinski-Harabasz Index, shown in the same vertical section as in Figure 5.

Table 1. Final parameters of local variograms obtained using the proposed method with the Silhouette Index

Zone	Nugget	Horizontal range (in grid blocks)	Vertical range (in grid blocks)
Top	0.69	25.94	6.48
Mid	0.54	23.19	5.80
Bottom	0.23	44.48	11.12

Table 2. Final parameters of local variograms obtained using the proposed method with the Davies-Bouldin Index

Zone	Nugget	Horizontal range (in grid blocks)	Vertical range (in grid blocks)
Top	0.71	22.74	5.68
Bottom	0.62	32.75	8.19

Table 3. Final parameters of local variograms obtained using the proposed method with the Calinski-Harabasz Index

Zone	Nugget	Horizontal range (in grid blocks)	Vertical range (in grid blocks)
Top	0.79	10.75	2.69
Mid-1	0.79	10.00	2.50
Mid-2	0.39	25.39	6.35
Bottom	0.23	44.49	11.12

The computation times for this application example—using SI, DB, and CH indices, respectively—were 4166, 3182, and 3539 seconds (measured over nine iterations, with 64 realizations generated per iteration) on an Intel Core i9 workstation with 32 GB of RAM. Among these, the

DB index resulted in the shortest computation time, followed by the CH index, while the SI index required the longest. However, considering both inversion accuracy and computational efficiency, the CH index demonstrated the best overall

performance, offering an optimal balance between accuracy and speed.

While the proposed method demonstrates strong performance, certain simplifications were intentionally incorporated to balance accuracy with computational efficiency, ensuring the method remains suitable for complex geological environments and practical for three-dimensional seismic inversion applications. The assumption of a fixed anisotropy ratio simplifies the modeling process and reduces computational demands, facilitating broader applicability, though it may not fully capture directional variations in highly heterogeneous settings. Additionally, while the Silhouette and Calinski-Harabasz indices provided robust clustering performance, the Davies-Bouldin Index showed less consistent results, highlighting that the choice of cluster validity indices can influence outcomes depending on data characteristics. Future research could focus on incorporating spatially varying anisotropy ratios and adaptive clustering validation techniques to further enhance the method's flexibility and robustness while maintaining reasonable computational costs.

#### 4. Conclusions

This work presented an iterative geostatistical seismic inversion approach designed to improve the estimation of petro-elastic properties in complex geological environments. The proposed method incorporates self-updating local variogram models, which are refined iteratively through automatic clustering to better represent local spatial variability. To determine the optimal number of clusters—and, by extension, the local variograms—the performance of three cluster validity indices, namely the Silhouette Index (SI), Davies-Bouldin Index (DB), and Calinski-Harabasz Index (CH), was compared within the framework of the proposed method. Validation was performed on a three-dimensional non-stationary synthetic dataset, demonstrating robust convergence when employing the SI and CH indices, with both achieving a high global correlation coefficient of 0.9 between the predicted and true seismic data. Among the tested indices, the CH index provided the most favorable balance of computational efficiency and inversion accuracy, making it the best performer in this application. Overall, the proposed method effectively captures local spatial continuity, delivering reliable results for complex subsurface modeling. Importantly, its successful application to three-dimensional

synthetic seismic data—with a reasonable computational cost—highlights its practical utility for real-world seismic inversion workflows in challenging geological settings.

#### Acknowledgments

The authors are grateful to Professor Amilcar Soares for his valuable suggestions and comments, which greatly improved this work. We also appreciate his generosity in providing the global stochastic inversion code and the synthetic dataset.

#### References

- [1] Bosch, M., Mukerji, T., & Gonzalez, E. F. (2010). Seismic inversion for reservoir properties combining statistical rock physics and geostatistics: A review. *Geophysics*, 75(5), 75A165-75A176.
- [2] Mohammadi, A. K., Mohebian, R., & Moradzadeh, A. (2021). High-resolution seismic impedance inversion using improved ceemd with adaptive noise. *Journal of Seismic Exploration*, 30(5), 481-504.
- [3] Tarantola, A. (2005). *Inverse problem theory and methods for model parameter estimation*. Society for industrial and applied mathematics.
- [4] Grana, D., Azevedo, L., De Figueiredo, L., Connolly, P., & Mukerji, T. (2022). Probabilistic inversion of seismic data for reservoir petrophysical characterization: Review and examples. *Geophysics*, 87(5), M199-M216.
- [5] Buland, A., & Omre, H. (2003). Bayesian linearized AVO inversion. *Geophysics*, 68(1), 185-198.
- [6] Grana, D., & Della Rossa, E. (2010). Probabilistic petrophysical-properties estimation integrating statistical rock physics with seismic inversion. *Geophysics*, 75(3), O21-O37.
- [7] Grana, D. (2016). Bayesian linearized rock-physics inversion. *Geophysics*, 81(6), D625-D641.
- [8] Grana, D., Fjeldstad, T., & Omre, H. (2017). Bayesian Gaussian mixture linear inversion for geophysical inverse problems. *Mathematical Geosciences*, 49, 493-515.
- [9] Azevedo, L., Narciso, J., Nunes, R., & Soares, A. (2021). Geostatistical seismic inversion with self-updating of local probability distributions. *Mathematical Geosciences*, 53(5), 1073-1093.
- [10] Azevedo, L., & Soares, A. (2017). *Geostatistical methods for reservoir geophysics* (Vol. 143). Salmon Tower Building, NY: Springer International Publishing.
- [11] Bortoli, L. J., Alabert, F., Haas, A., & Journel, A. (1993). Constraining stochastic images to seismic data: Stochastic simulation of synthetic seismograms.

In *Geostatistics Tróia '92: Volume 1* (pp. 325-337). Dordrecht: Springer Netherlands.

[12] Durrani, M. Z., Talib, M., Ali, A., Sarosh, B., & Rahman, S. A. (2021). Characterization of carbonate reservoir using post-stack global geostatistical acoustic inversion approach: A case study from a mature gas field, onshore Pakistan. *Journal of Applied Geophysics*, 188, 104313.

[13] Haas, A., & Dubrule, O. (1994). Geostatistical inversion-a sequential method of stochastic reservoir modelling constrained by seismic data. *First break*, 12(11).

[14] Pereira, Â., Azevedo, L., & Soares, A. (2023). Updating local anisotropies with template matching during geostatistical seismic inversion. *Mathematical Geosciences*, 55(4), 497-519.

[15] Soares, A., Diet, J. D., & Guerreiro, L. (2007). Stochastic inversion with a global perturbation method. *Petroleum geostatistics. Cascais, Portugal: EAGE*.

[16] Nunes, R., Soares, A., Azevedo, L., & Pereira, P. (2017). Geostatistical seismic inversion with direct sequential simulation and co-simulation with multi-local distribution functions. *Mathematical Geosciences*, 49, 583-601.

[17] Sabeti, H., Moradzadeh, A., Ardejani, F. D., Azevedo, L., Soares, A., Pereira, P., & Nunes, R. (2017). Geostatistical seismic inversion for non-stationary patterns using direct sequential simulation and co-simulation. *Geophysical Prospecting*, 65, 25-48.

[18] Sevilla-Villanueva, B., Gibert, K., & Sánchez-Marré, M. (2016, September). Using CVI for understanding class topology in unsupervised scenarios. In *Conference of the Spanish Association for Artificial Intelligence* (pp. 135-149). Cham: Springer International Publishing.

[19] Abdalameer, A. K., Alswaiti, M., Alsudani, A. A., & Isa, N. A. M. (2022). A new validity clustering index-based on finding new centroid positions using the mean of clustered data to determine the optimum number of clusters. *Expert Systems with Applications*, 191, 116329.

[20] Arbelaitz, O., Gurrutxaga, I., Muguerza, J., Pérez, J. M., & Perona, I. (2013). An extensive comparative study of cluster validity indices. *Pattern recognition*, 46(1), 243-256.

[21] José-García, A., & Gómez-Flores, W. (2021). A survey of cluster validity indices for automatic data clustering using differential evolution. In *Proceedings of the genetic and evolutionary computation conference* (pp. 314-322).

[22] Ikotun, A. M., Habyarimana, F., & Ezugwu, A. E. (2025). Cluster validity indices for automatic clustering: A comprehensive review. *Heliyon* 11: e41953.

[23] Soares, A. (2001). Direct sequential simulation and cosimulation. *Mathematical Geology*, 33, 911-926.



دانشگاه صنعتی شاهرود

# نشریه مهندسی معدن و محیط زیست

www.jme.shahroodut.ac.ir نشانی نشریه:



انجمن مهندسی معدن ایران

## مدل‌های واریوگرام محلی خودبه‌روز شونده با استفاده از خوشه‌بندی خودکار در وارون‌سازی لرزه‌ای زمین آماری تکراری

شقایق اسماعیل زاده<sup>۱</sup>، علی مرادزاده<sup>۱\*</sup>، رضا محبیان<sup>۱</sup> و امید اصغری<sup>۱</sup>

دانشکده مهندسی معدن، دانشکده‌گان فنی، دانشگاه تهران، تهران، ایران

### چکیده

وارون‌سازی لرزه‌ای یک روش با اهمیت برای تخمین توزیع فضایی خواص پتروالاستیک در زیر سطح زمین، بر اساس داده‌های بازتاب لرزه‌ای است. این پژوهش یک روش وارون‌سازی لرزه‌ای زمین آماری تکراری را معرفی می‌کند که با هدف رفع چالش‌های موجود در محیط‌های زمین‌شناسی پیچیده، از مدل‌های واریوگرام محلی خودبه‌روز شونده استفاده می‌کند. برخلاف روش‌های مرسوم که به یک واریوگرام کلی یا واریوگرام‌های محلی ثابت متکی هستند، این روش به‌طور پویا مدل‌های پیوستگی فضایی را در هر تکرار با استفاده از مدل‌سازی خودکار واریوگرام و خوشه‌بندی پارامترهای واریوگرام به‌روزرسانی می‌کند. تعداد بهینه خوشه‌ها با استفاده از سه شاخص اعتبارسنجی بنام شاخص سیلوئت (SI)، شاخص دیویس-بولدن (DB) و شاخص کالینسکی-هاراباس (CH) تعیین می‌شوند. کارایی این روش با استفاده از یک مجموعه داده مصنوعی سه‌بعدی غیرایستا ارزیابی شد و نشان داده شد که روش با استفاده از شاخص‌های SI و CH به همگرایی قوی دست یافته است، به‌طوری که روش معرفی شده با هر دو شاخص به ضریب همبستگی کلی بالای ۰.۹ بین داده‌های لرزه‌ای پیش‌بینی‌شده و واقعی رسیدند. در میان این شاخص‌ها، شاخص CH بهترین تعادل را بین کارایی محاسباتی و دقت وارون‌سازی ارائه داد. نتایج نشان می‌دهد که این روش توانایی بالایی در ثبت تغییرات فضایی محلی دارد، در حالی که هزینه محاسباتی معقولی را حفظ می‌کند و آن را به یک رویکرد امیدوارکننده برای وارون‌سازی لرزه‌ای در محیط‌های زیرسطحی پیچیده تبدیل می‌کند.

### اطلاعات مقاله

تاریخ ارسال: ۲۰۲۵/۱۱/۰۳

تاریخ داوری: ۲۰۲۵/۰۲/۱۷

تاریخ پذیرش: ۲۰۲۵/۰۲/۰۶

DOI: 10.22044/jme.2025.15541.2978

### کلمات کلیدی

وارونگی تصادفی  
مدل‌های پیوستگی مکانی محلی  
شبیه‌سازی متوالی مستقیم  
خودآموز  
خوشه‌بندی سلسله مراتبی